EXTENSION OF THE NAVAL SPACE COMMAND SATELLITE THEORY PPT2 TO INCLUDE A GENERAL TESSERAL M-DAILY MODEL

by

P. J. Cefola[1] and D. J. Fonte[2]

ABSTRACT

The Naval Space Command PPT2 model of satellite motion has been used for 30 years to maintain a catalog of Earth satellites. The PPT2 algorithm is based on Brouwer's 1959 artificial satellite theory and includes the Lyddane modification for small eccentricity and inclination and a separate modification for the critical inclination. In this paper, the authors describe a modified version of PPT2 which includes a recursive analytical model for the portion of the tesseral harmonic perturbation that depends on just the Greenwich hour angle. These tesseral m-daily terms are the major source of unmodeled periodic motion in PPT2 for many LEO satellite orbits. The recursive tesseral model is drawn from the Draper Semianalytical Satellite Theory (DSST) and provides the short-period variations in terms of the equinoctial elements [tan(i/2) convention]. Modifications to the Lyddane expressions which allow the double-primed elements to be converted to single-primed and osculating (including the J2 short periodics) equinoctial elements are introduced. The software intricacies of accessing the DSST m-daily model from the R&D GTDS version of PPT2 are addressed. Numerical comparisons of the PPT2-MDAILY algorithm with the DSST suggest that the additional errors of commission are negligible. Numerical tests with DSST as a reference are also employed to demonstrate the errors associated other unmodeled perturbations (zonal short periodics other than J2, tesseral linear combination short periodics, unmodeled zonal terms in the secular and long periodic motion, etc.). Numerical test results with Cowell as a reference are consistent with the DSST-based testing. Very high precision, externally generated reference orbits for TOPEX and TAOS are used to demonstrate the accuracy improvement associated with PPT2-MDAILY.

---

1 Senior Member, AIAA. Program Manager for Astrodynamic Applications, The Charles Stark Draper Laboratory, Cambridge, MA. Also Lecturer in Aeronautics and Astronautics, MIT.

2 U. S. Air Force.

INTRODUCTION

The Naval Space Command PPT2 model of satellite motion (Refs. 1 and 2) has been used for about 30 years to maintain a catalog of Earth satellites. The PPT2 algorithm is based on Brouwer's 1959 artificial satellite theory and is a contemporary of the Air Force Space Command GP theories SGP and GP4 (Ref. 3). Accuracy and compatibility requirements continue to evolve (Ref. 4) and the Naval Space Command is presently testing an improved theory which adds the DP4 "deep space" terms (Ref. 5) to PPT2; this new theory is called PPT3 (Ref. 6). The Navy is also supporting the development of a more advanced, purely analytical theory (Ref. 7) as well as investigating orbit determination based on purely numerical means (Ref. 8).

In 1995 the authors implemented the PPT2 theory within the workstation/PC version of the GTDS Orbit Determination Program (Ref. 9). The numerical testing of the GTDS PPT2 implementation included Differential Correction (DC) runs in which the PPT2 theory was least squares fit to either simulated or real data. Of these, the most interesting runs were those in which PPT2 was fit to Precise Orbit Ephemeris (POE) data for the TOPEX and TAOS spacecraft. The TOPEX POE data is unique in that it provides position data that is accurate to 15 cm over the whole orbit. This very high orbit accuracy is the result of accurate, temporally dense, and globally distributed tracking data (satellite laser ranging and DORIS receiver), and the application of improved satellite force models (Ref. 10). For the lower altitude TAOS, the POE data is based on Differential GPS processing; the TAOS POE orbits are believed to be accurate to about three (3) meters (Ref. 11).

The comparisons between the best fit PPT2 trajectories and the POE trajectories provide new insight into the inherent accuracy of the PPT2 model. Figures 1 and 2 show

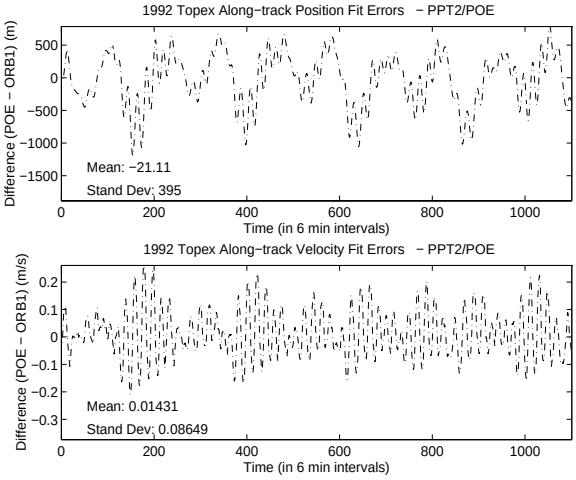

Figure 1. Along Track Differences, Best Fit PPT2 vs. TOPEX POE

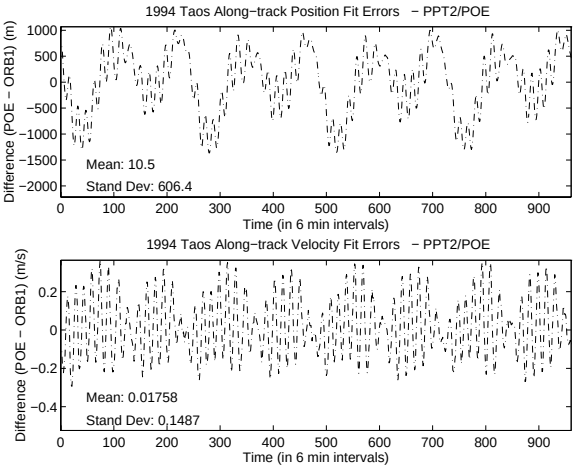

Figure 2. Along Track Differences, Best Fit PPT2 vs. TAOS POE

the along track differences for the TOPEX and TAOS cases, respectively. The TOPEX fit span is about 4.6 days and TAOS fit span is 4 days. Inspection of these differences shows high frequency oscillations with periods near the orbital period and longer period oscillations with periods near 12 and 24 hours. In fact, the 12 and 24 hour oscillations are the major error in the along track position residuals. This conclusion is supported by similar plots for the orbital elements. This conclusion is also supported by a simulated data case [see Table 5 in Ref. 9].

In this paper, the authors extend the PPT2 theory to include a general recursive tesseral m-daily model. The goal is to address the tesseral m-daily errors observed in Figures 1 and 2 without significantly increasing the complexity of the algorithm. We name the new theory PPT2-MDAILY. The recursive tesseral m-daily model is taken from the Draper Semianalytical Satellite Theory (DSST) (Ref. 12).

Subsequent sections of the paper describe:

- Mathematical Considerations for PPT2-MDAILY
- GTDS PPT2-MDAILY Software Design
- Numerical Testing of GTDS PPT2-MDAILY

- Conclusions and Future Work

MATHEMATICAL CONSIDERATIONS FOR PPT2-MDAILY

This section has three goals:

1. to review the Brouwer-Lyddane theory
2. to focus on the periodic recovery process employed in the PPT2 theory
3. to introduce the new expressions employed in the PPT2-MDAILY theory

The Naval Space Command PPT2 model of satellite motion is based on the work of Brouwer (Refs. 13 and 14). The Brouwer theory accounts for gravitational effects of the zonal harmonics J_2, J_3, J_4, and J_5. These effects, which are separated into secular, long period, and short period contributions, are modeled to low order. PPT2 also includes the Lyddane modification to account for singularities which arise in the Brouwer equations of motion for zero eccentricity and zero inclination, while other modifications are made to address the singularities at the critical inclination (Ref. 1).

The Brouwer equations of motion are based on the canonical Delaunay element set

$L = (\mu a)^{1/2}$ l = mean anomaly

$G = L\,(1 - e^2)^{1/2}$ g = argument of perigee (1)

$H = G \cos I$ h = longitude of ascending node

and take the following form:

$$\dot{L} = \frac{\partial F}{\partial l} \qquad \dot{l} = -\frac{\partial F}{\partial L}$$
$$\dot{G} = \frac{\partial F}{\partial g} \qquad \dot{g} = -\frac{\partial F}{\partial G} \qquad (2)$$
$$\dot{H} = \frac{\partial F}{\partial h} \qquad \dot{h} = -\frac{\partial F}{\partial H}$$

where:

a is the semimajor axis

e is the eccentricity

I is the inclination

μ is the gravitational parameter

F is the Hamiltonian = $U - 0.5v^2$, in which

U is the gravitational potential for a non-spherical earth

v is the velocity

The solution of Eq. (2) proves quite challenging due to the complex nature of the Hamiltonian (which is a function of L, G, H, l, and g; it is not a function of h). However, these expressions can be simplified if the variables are transformed such that the resulting Hamiltonian is independent of some of the new variables. In this manner, the solution to the transformed equations of motion leads to a subset of the variables remaining constant, while the remaining variables vary linearly with time.

Brouwer implements two transformations. The doubly transformed elements are referred to as double primed elements (i.e., L", G", H", l", g", and h"). These elements, which Brouwer also calls mean elements, contain only secular contributions from the gravitational perturbation. As it turns out, L", G", and H" are the subset of elements which remain constant, while l", g", and h" can be expressed as linear functions of time. If L", G", and H" are constant, then the double primed elements a", e", and I" are also constant (in other words, semimajor axis, eccentricity, and

inclination experience no secular variation from the geopotential). Starting with a given set of initial Brouwer mean elements, expressions for l'' , g", and h" take the following form:

$$\begin{aligned} l'' &= l''_o + n_o t\,(1 + \delta l_{sec}) \\ g'' &= g''_o + n_o t\,\delta g_{sec} \\ h'' &= h''_o + n_o t\,\delta h_{sec} \end{aligned} \qquad (3)$$

where the $_o$ subscript refers to the initial value of the mean element, t is time, $\delta element_{sec}$ is the secular contribution to the given element, and $n_o = (\mu/a''^3)^{1/2}$, is the mean motion computed from the mean semimajor axis. As mentioned previously, the other mean elements remain equal to their initial values:

$$\begin{aligned} a'' &= a''_o \\ e'' &= e''_o \\ I'' &= I''_o \end{aligned} \qquad (4)$$

Brouwer makes a distinction between long period and short period contributions of the geopotential; long period terms contain the argument of perigee (g) in their argument, while short period terms contain the mean anomaly in their argument (or combinations of l with other variables, such as g). The Brouwer single primed elements (i.e., l', g', and h', as well as a', e', and I') contain secular (if applicable) and long period perturbing effects of the geopotential. However, care must used when computing the Brouwer periodic contributions to the elements. The expressions for the long period terms contain divisors which go to zero for values of eccentricity and inclination equaling zero, as well as for inclinations equaling the *critical* value. The Lyddane modification, which uses mean elements in the computation of short periodic quantities (rather than single primed elements), as well as a variation of the Delaunay element set, is used to address the singularities for zero values of eccentricity and inclination. Other modifications have been added to PPT2 to account for the critical inclination problem (Ref. 1).

The periodic recovery process in PPT2 is organized around the computation of the following intermediate quantities:

$$DE = e'' + \delta_1 e + \delta_2 e + AGDE$$

$$DI = \sin\frac{1}{2} I'' + \left(\cos\frac{1}{2} I''\right)\frac{1}{2}(\delta_1 I + \delta_2 I + AGDI)$$

$$DH = \left[(\sin I'')(\delta_1 h + \delta_2 h) + AGDH\right] / (2\cos\frac{1}{2} I'') \qquad (5)$$

$$DL = e''\delta_1 l + e''\delta_2 l + AGDL$$

$$OS = l'' + g'' + h'' + \delta_1 z + \delta_2 z + AGDG$$

$$a = a'' + \delta_2 a + AGDA$$

The definition of these quantities is motivated by Eq. (15) in Ref. 1. In Eq. (5), the δ_1 terms are the long periodics [see Eq. (25) through Eq. (29) in Ref. 1] and the δ_2 terms are the short periodics [see Eq.(36) through Eq.(41) in Ref. 1]. The quantities AGDi in Eq.(5) are the optional PPT2 corrections. These are not considered further in the present work; they are set equal to zero.

Next, the following nonsingular quantities are computed:

$$e\cos l = DE\cos l'' - DL\sin l''$$

$$e\sin l = DE\sin l'' + DL\cos l''$$

$$(\sin\frac{1}{2} I)\cos h = DI\cos h'' - DH\sin h'' \qquad (6)$$

$$(\sin\frac{1}{2} I)\sin h = DI\sin h'' + DH\cos h''$$

Equation (6) is equivalent to Eq.(15) in Ref. 1. The left hand sides of these equations are osculating quantities including both the long and short periodic effects. These equations are easily solved for the osculating Keplerian elements.

For the PPT2-MDAILY theory developed in this paper, two additional outputs from PPT2 are required. These are:

1. The single-primed equinoctial elements at an arbitrary request time
2. The osculating equinoctial elements including the J2 short periodics at an arbitrary request time

The equinoctial elements have the following definitions in terms of the Keplerian elements:

$$\begin{aligned} a &= a \\ h &= e\sin(\omega+\Omega) \\ k &= e\cos(\omega+\Omega) \\ p &= \tan(i/2)\sin\Omega \\ q &= \tan(i/2)\cos\Omega \\ \lambda &= M+\omega+\Omega \end{aligned} \tag{7}$$

The single-primed equinoctial elements will be used in place of the DSST mean equinoctial elements as an input to the computation of the tesseral m-daily Fourier coefficients. This process will result in interpolators for the tesseral m-daily coefficients which are valid for a multiple day interval. These interpolators can be refreshed as required in the PPT2-MDAILY output at request time function.

The computation of the osculating equinoctial elements including the J2 short periodics is part of the strategy for assembling osculating equinoctial elements which include both the J2 *and* tesseral m-daily short periodics.

To compute the osculating equinoctial elements [defined in Eq. (7)] including the J2 short periodics, Eq. (6) and the subsequent analytic solution are replaced with

$$
\begin{aligned}
a &= a'' + \delta_2 a \\
e\sin(\omega+\Omega) &= DE\sin(OS-l'') - DL\cos(OS-l'') \\
e\cos(\omega+\Omega) &= DE\cos(OS-l'') + DL\sin(OS-l'') \\
\tan(i/2)\sin\Omega &= \frac{DI\sin(h'') + DH\cos(h'')}{\sqrt{1-DI^2-DH^2}} \\
\tan(i/2)\cos\Omega &= \frac{DI\cos(h'') - DH\sin(h'')}{\sqrt{1-DI^2-DH^2}} \\
M+\omega+\Omega &= l''+g''+h''+\delta_1 z+\delta_2 z
\end{aligned}
\tag{8}
$$

The equations for $e\sin(\omega+\Omega)$ and $e\cos(\omega+\Omega)$ are obtained by straightforward algebraic manipulation of Eqs. (5) and (6). The term $OS-l''$ in Eq. (8) is evaluated via the expression

$$
OS - l'' = g'' + h'' + \delta_1 z + \delta_2 z \tag{9}
$$

To compute the single-primed equinoctial elements, we truncate Eq.(5) so that the J2 short periodics are not included. The new result is

$$
\begin{aligned}
DE &= e'' + \delta_1 e \\
DI &= \sin\frac{1}{2}I'' + \left(\cos\frac{1}{2}I''\right)\frac{1}{2}(\delta_1 I) \\
DH &= \left[(\sin I'')(\delta_1 h)\right]/(2\cos\frac{1}{2}I'') \\
DL &= e''\delta_1 l \\
OS &= l''+g''+h''+\delta_1 z \\
a &= a''
\end{aligned}
\tag{10}
$$

These equations can be used in the right hand sides of Eq. (8) to produce the single primed equinoctial elements. The only modification is that the term $OS-l''$ is given by

$$
OS - l'' = g'' + h'' + \delta_1 z \tag{11}
$$

For the PPT2-MDAILY theory, it is assumed that the Brouwer single primed equinoctial elements *directly correspond* to the DSST mean equinoctial elements. With the DSST mean equinoctial elements available, the tesseral m-daily short periodic contributions for each equinoctial element (η_i, where i represents the particular equinoctial element) can be computed by:

$$\eta_i = \sum_{j=1}^{j\max} \left[C_i^j(a,h,k,p,q,t)\cos(j\theta) + S_i^j(a,h,k,p,q,t)\sin(j\theta) \right] \qquad (12)$$

In Eq. (12), the Fourier coefficients C and S are functions of the first five, mean equinoctial elements and time. The quantity θ in Eq.(12) represents the Greenwich hour angle.

To make the tesseral m-daily computation more efficient, the Fourier coefficients C and S in Eq.(12) are computed at a few, equally-spaced time points. Using these values, Lagrange interpolators for the C and S coefficients are constructed. It is the interpolators for the C and S coefficients that are employed at each output request time.

The PPT2-MDAILY output at request time functionality can be summarized as follows:

1. Compute the equinoctial elements including the J2 short-periodics via equations (5) and (8)
2. Compute the tesseral m-daily corrections to the equinoctial elements via equation (12)
3. Sum the two contributions to obtain the osculating equinoctial elements
4. Convert the osculating equinoctial elements to position and velocity via the two-body mechanics expressed in terms of the equinoctial elements

GTDS PPT2-MDAILY SOFTWARE DESIGN

The purpose of this development is to establish the capability to exercise the PPT2 theory in conjunction with a subset of the DSST short periodic models. Here, the DSST short

periodic model is considered to include both the package for managing the short periodic coefficient interpolators (subroutines SPGENR, SPCOEF, SPMOVE, SPINTP, etc.) and the detailed astrodynamic models for the short periodic coefficients (SPZONL, SPMDLY, SPJ2MD, SPTESS, etc.). The DSST also includes two key common blocks: /SPINTG/ and /SPREAL/. Common block /SPINTG/ includes the integer flags for controlling the DSST short periodic model and /SPREAL/ includes all the real variables (including the interpolator coefficients) associated with the short-periodic models. Both of these common blocks are configured to support the complete DSST short periodic model. With this background, three design concepts evolved:

1. a simple implementation which allowed subroutine PPT2 to make a direct call to the detailed tesseral m-daily model (subroutine SPMDLY)

2. a more operationally-oriented implementation in which the DSST routines for managing the short periodic coefficient interpolators and the associated common blocks /SPINTG/ and /SPREAL/ are replaced with modules tailored to a PPT2 tesseral m-daily only capability

3. a design in which just the drivers for the DSST short-periodic model truncation, interpolator coefficient generation, and application are replaced with drivers tailored to PPT2

The first concept had the advantages of requiring minimal software development and being self-contained. However, it did not include the short-periodic coefficient interpolator concept. As a result, the computational speed of this concept would not represent fairly the true capability of the PPT2-MDAILY theory. The second concept required the most software development of the three. It does have the advantage that the product could be implemented more easily in a non-GTDS environment.

The third concept requires moderate software development; however, the predominant portion of the DSST package for managing the short periodic coefficient interpolators is unmodified. Thus the third concept offers the most flexibility in experimenting with the PPT2/DSST short periodic hybrid satellite theory. This is the concept that has been adopted in the present exploratory development.

Figure 3 gives an overview of the present GTDS PPT2-MDAILY capability.

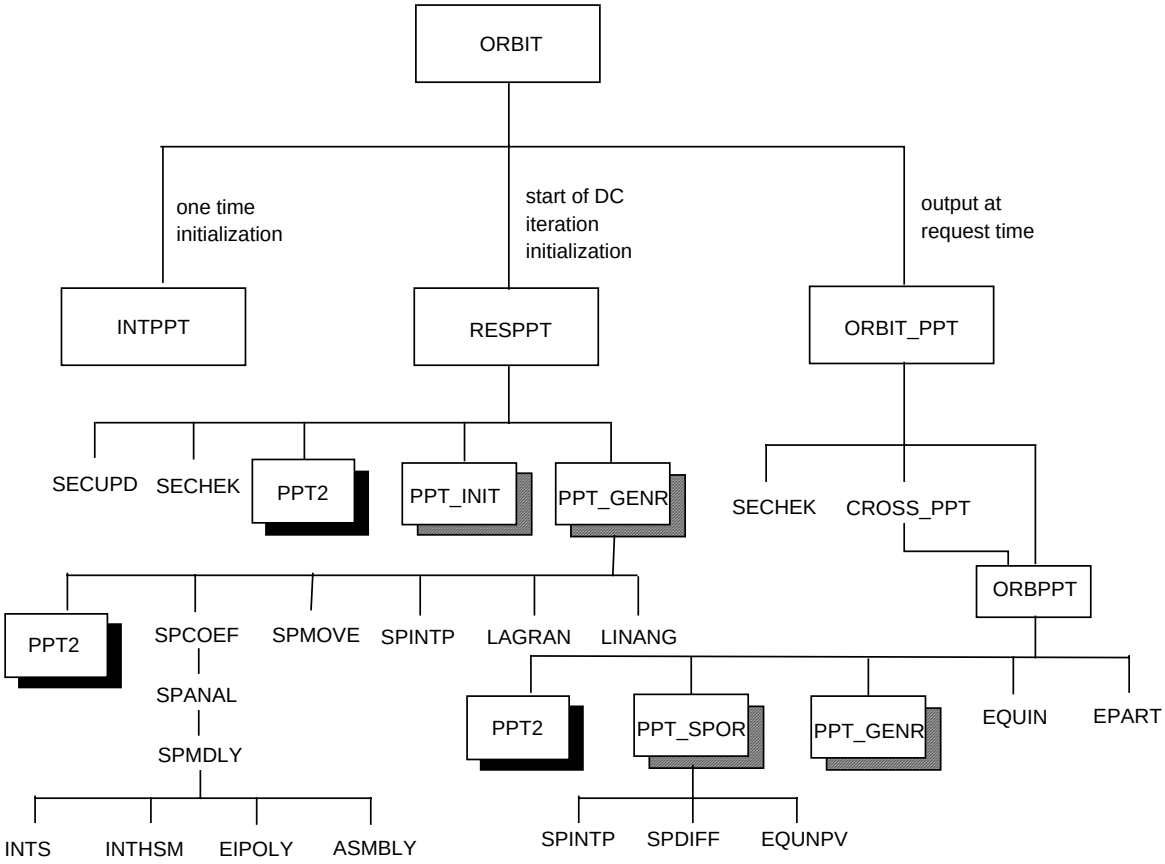

Figure 3. GTDS PPT2-MDAILY Software Architecture

Overall, eight (8) existing GTDS modules were modified and three (3) new modules were created. The new modules are:

- PPT_INIT
- PPT_GENR
- PPT_SPOR

Subroutine PPT_INIT sets the DSST short-periodic switches so that only the tesseral m-daily model is exercised with the desired geopotential degree and order and coefficient interpolator configuration. Subroutine PPT_GENR is called by the RESPPT to compute the first tesseral m-daily coefficient interpolator. Nominally, this interpolator would be valid for a multiple

day interval. Subroutine PPT_GENR is also called by ORBPPT in case the tesseral m-daily coefficient interpolator needs to be refreshed. A primary difference between PPT_GENR and its DSST analog (SPGENR) is that PPT_GENR calls PPT2 to obtain the single-primed equinoctial elements on the short periodic coefficient grid. The single-primed elements are the input to SPCOEF (taking the place of the DSST mean elements in that theory). Subroutine PPT_SPOR constructs the osculating equinoctial elements including both the J2 short periodics and tesseral m-daily terms and the corresponding perturbed position and velocity. Subroutine PPT_SPOR calls SPINTP to evaluate the tesseral m-daily coefficient interpolators at the output request time and then subroutine SPDIFF to assemble the m-daily short periodic variations in the equinoctial element space. These variations are added to the J2 osculating elements computed within subroutine PPT2. Finally, PPT_SPOR calls EQUNPV to convert the osculating equinoctial elements to position and velocity.

The eight (8) modified modules are:

- SETORB
- SETOG1
- PPTELSBD
- CENANG
- RESPPT
- ORBPPT
- PPT2
- PPTPARBD

Modules SETORB, SETOG1, and PPTELSBD (block data for common /PPTELS/) were modified to support additional input data options for the PPT2-MDAILY theory. Subroutine CENANG is used to set the physical constants and orientation angles of the central body in the DSST short periodic model; CENANG was modified to support the NORAD True of Reference

integration coordinate system employed by PPT2. RESPPT and ORBPPT were modified to make the calls to the new subroutines PPT_INIT, PPT_GENR, and PPT_SPOR. The core subroutine PPT2 was modified to output single primed and osculating equinoctial elements at each output request time. Common block /PPTPAR/ (described in module PPTPARBD) was modified to support communication of the single primed and osculating equinoctial elements. The original development of RESPPT and ORBPPT is described in Ref. 9.

The development and testing described in this paper have been accomplished in a PC computing environment. Both a Winbook XP 486 PC-compatible notebook and a Gateway 2000 Pentium PC-compatible desktop platform have been employed.

NUMERICAL TESTING OF GTDS PPT2-MDAILY

Testing of the GTDS PPT2-MDAILY Capability with Truth Data Generated by the Draper Semianalytic Satellite Theory (DSST)

As discussed in the preceding paper (Ref. 9), testing a perturbation theory against a reference theory with equivalent physical force models is a well established procedure for verifying that the perturbation theory correctly includes those effects considered in the theory development (Refs. 15-18). In this subsection, various test cases are presented in which the GTDS PPT2-MDAILY and GTDS PPT2 theories are least squares fit to reference orbits generated with the DSST. DSST has been chosen to generate the reference orbits since its perturbation models (geopotential, drag, third body, and solar radiation pressure) can easily be separated into secular/long period, and short period contributions. The ability to analyze each subset of the zonal and tesseral harmonics (resonance, m-dailies, and linear combination terms) independently and to an arbitrary degree and order is particularly useful.

For the first test case, initial conditions matching those employed in the original GTDS PPT2 test process (see Ref. 9, Figure 15) are used in the generation of the truth trajectory. The chosen DSST mean elements correspond to a near circular, 450 km orbit inclined at 75 degrees. The Test Case 1 Truth Model Parameters are given in Table 1.

Table 1. Test Case 1 Truth Model Parameters

Parameter	Value	Parameter	Value
Epoch (YYMMDD.0)	820223.0	Epoch (HHMMSS.S)	000000.0
Input Coordinate Frame	GTDS True of Date	Atmospheric Drag	No
Input Element Type	DSST Average (Mean) Keplerian	Solar Radiation Pressure	No
Semimajor Axis	6835.0814 km	Third Body Point Mass	No
Eccentricity	0.0010201164	Gravitational Parameter	398597.63 km^3/sec^2
Inclination	74.9567 deg	Gravity Model	WGS 72
Longitude of Ascending Node	228.6393 deg	DSST Step Size	43200 sec
Argument of Perigee	271.2229 deg	Integration Coordinate Frame	GTDS Mean of 1950
Mean Anomaly	88.164558 deg	Output Coordinate Frame	GTDS Mean of 1950

The DSST force models used in the truth ephemeris for Test Case 1 are chosen to include those terms that PPT2-MDAILY models exactly:

TEST # 1

Mean Element Equations of Motion

- 5 x 0 zonal harmonics
- J_2^2 terms

Short Periodics

- J_2 terms
- Tesseral M-daily terms (through degree and order 5)[3]

[3] The exact solution for the tesseral m-daily Fourier coefficients corresponding to the 5x5 terms implements eccentricity to the 3rd power

The next step in the process is to fit both PPT2 and PPT2-MDAILY to the DSST truth data. The initial conditions for the least squares fit to the DSST truth trajectory are given in Table 2.

Table 2. Test Case 1 PPT2/PPT2-MDAILY DC Input Parameters

Parameter	Value	Parameter	Value
Epoch (YYMMDD.0)	820223.0	Epoch (HHMMSS.S)	000000.0
Input Coordinate Frame	GTDS NORAD TEME	Fit Span Length	3 Days
Input Element Type	PPT2 Mean Keplerian	Solve for M_2	No
Semimajor Axis	6835.08 km	Solve for M_3	No
Eccentricity	0.001	Gravitational Parameter	398597.63 km^3/sec^2
Inclination	74.95 deg	Gravity Model	WGS 72
Longitude of Ascending Node	228.6393 deg	M-daily Terms	Through Degree and Order 5
Argument of Perigee	271.2 deg	Position Observation σ	1500 m
Mean Anomaly	88.16 deg	Velocity Observation σ	150 cm/sec
M_2	0.0 rad/$Herg^2$	Integration Coordinate Frame	GTDS NORAD TEME
M_3	0.0 rad/$Herg^3$	Output Coordinate Frame	GTDS Mean of 1950

The results of the least squares fits to the truth data are given in Table 3.

Table 3. Test Case 1 PPT2/PPT2-MDAILY DC Results

Parameter	GTDS PPT2 (Original)	GTDS PPT2-MDAILY
Run Time	38.34 sec	41.25 sec
DC RMS	595.30 m	15.35 m
DC Iterations	6	5
Semimajor Axis σ	8.01907 cm	0.210646 cm
Total Position Error RMS* 3 Day Fit	611.62 m	15.271 m
Total Position Error RMS* 3 Day Predict	628.79 m	15.872 m

In Table 3, the Total Position Error RMS is a product of the GTDS Compare Program. The difference between the DC RMS and the Total Position Error RMS (3 day fit) is the number of comparison points used in the generation of the metric (the Compare Program was configured to use fewer comparison points than the DC RMS calculation; the DC RMS calculation used one point every 450 seconds, while the Compare Program used one point every 2700 seconds). All timing metrics in this paper were obtained via a call to an internal clock routine immediately prior to and subsequent to program execution on the Gateway 2000 Pentium PC.

These results indicate a 15.35 m difference between the truth model and PPT2 MDAILY theory. When the original GTDS PPT2 theory was fit to a DSST truth model containing these same force models except the m-dailies (i.e., the force models in the DSST truth and GTDS PPT2 were nearly identical, see Ref. 9: Table 1), a 15.24 m error resulted. This indicates negligible additional error of commission was introduced through the attachment of the m-daily model to GTDS PPT2. Thus we claim that the m-daily model was properly attached to GTDS PPT2.

The improvement gained by using the m-daily model can be seen clearly in Table 3; the magnitude of the DC RMS is reduced by over 500 m (an error nearly 40 times smaller). An analysis of element difference plots between the truth and GTDS PPT2 trajectories exhibits the 12 and 24 hour frequency oscillations characteristic of the m-dailies. These error signatures are not evident in the difference plots between GTDS PPT2 M-DAILY and the truth trajectory. This improvement was gained at the expense of a 7.5 % increase in run time.

The next several test cases incrementally add other perturbation effects to the DSST truth model. Because these effects are not modeled in PPT2-MDAILY, the differences between the best fit PPT2-MDAILY trajectory and the DSST truth are generally larger than in Table 3. These cases allow an assessment of the desirability of adding additional classes of terms to the PPT2-MDAILY theory. Table 4 lists the error sources considered in each test case.

Table 4. Error Sources by Test Case

Test Case No.	Error Sources Considered
2	J3, J4, J5 short periodics
3	J3, J4, J5 short periodics 5 x 5 Tesseral Linear Combination Terms
4	J3, J4, J5 short periodics 5 x 5 Tesseral Linear Combination Terms J2-squared short periodics
5	J3, J4, J5 short periodics 5 x 5 Tesseral Linear Combination Terms J2-squared short periodics J2/m-daily coupling
6	J6,...,J12 secular and long periodic terms

7	secular, long periodic, and short periodic effects due to Jacchia 1970 density model with fixed F10.7 and Ap

For Test Case 2, the initial conditions from the first test case were used to generate the truth trajectory. For this test, however, a full zonal short periodic model was included in the DSST truth generation:

TEST # 2

Mean Element Equations of Motion

- 5 x 0 zonal harmonics
- J_2^2 terms

Short Periodics

- Zonal terms through degree 5[4]
- Tesseral M-daily terms (through degree and order 5)

The initial conditions for the least squares fit to this truth trajectory are the same as those given in Table 2 for the first test case. The results of the differential correction runs for the second test case are given in Table 5.

Table 5. Test Case 2 PPT2/PPT2-MDAILY DC Results

Parameter	GTDS PPT2 (Original)	GTDS PPT2-MDAILY
Run Time	37.76 sec	39.44 sec
DC RMS	595.28 m	14.44 m

[4] Zonal short periodics through degree 5 implement eccentricity to the 4^{th} power and 11 frequencies in the true longitude

DC Iterations	6	5
Semimajor Axis σ	8.01837 cm	0.174895 cm
Total Position Error RMS 3 Day Fit	611.61 m	14.278 m
Total Position Error RMS 3 Day Predict	629.41 m	15.072 m

The results for this particular test case are inconclusive with regards to the zonal short periodic model; it is expected their impact would be small. However, it would be best to analyze the impact of the zonal short periodics across a spectrum of different orbits (especially near earth orbits with different inclinations and eccentricities). For this particular test case, it could be concluded the extra computational expense is not worth the accuracy difference.

The next run (Test Case 3) adds tesseral linear combination short periodics to the DSST truth trajectory (other initial conditions for the DSST truth remain the same as in the first two test cases):

TEST # 3

Mean Element Equations of Motion

- 5 x 0 zonal harmonics
- J_2^2 terms

Short Periodics

- Zonal terms through degree 5
- Tesseral M-daily terms (through degree and order 5)
- Tesseral linear combination short periodics (through degree and order 5)[5]

[5] Tesseral linear combination terms through degree and order 5 implement eccentricity squared to the 2nd power (d'Alembert characteristic to the 4th power) and frequencies in the mean longitude ranging from -9 to 9

The initial conditions for the least squares fit to this truth trajectory are the same as those given in Table 2 for the first (and second) test case. The results of the differential correction runs for the third test case are given in Table 6.

Table 6. Test Case 3 PPT2/PPT2-MDAILY DC Results

Parameter	GTDS PPT2 (Original)	GTDS PPT2-MDAILY
Run Time	38.06 sec	38.28 sec
DC RMS	606.43 m	53.09 m
DC Iterations	6	4
Semimajor Axis σ	8.10886 cm	0.778215 cm
Total Position Error RMS 3 Day Fit	623.30 m	52.332 m
Total Position Error RMS 3 Day Predict	643.04 m	53.414 m

Based on these results, it can be concluded that the tesseral linear combination short periodics account for about another 40 meters worth of accuracy (in a one sigma sense). This contribution mainly surfaces in the fit span due to the periodic nature of the tesseral short periodics; no dominant secular increase in error is evident in the predict span. For potential applications like catalog maintenance with a large number of space objects, the increased computational expense required to include the tesseral short periodics is not worth the accuracy improvement gained (keep in mind the timing metrics presented in Table 6 are somewhat misleading since the GTDS PPT2-MDAILY theory converged in 4 iterations while the GTDS PPT2 theory took 6 iterations). However, for applications requiring the best available force models and high accuracy, the tesseral short periodics are a necessity.

The next test case added J_2^2 short periodic terms (Test Case 4) to the DSST truth model, followed by J_2 m-daily coupling short periodic terms (Test Case 5). In this manner, the DSST's geopotential model was complete through degree and order five (DSST's best emulation of a 5x5 Special Perturbations/numerical integration technique). For both of these test cases, the DC RMS was approximately 53 meters. Since it was already proven the zonal short periodics spanning J_3 to J_5 did not particularly impact accuracy for these initial conditions, it was not expected that other terms of this order (i.e., J_2^2 and J_2 m-daily) would significantly impact accuracy. In general, an analysis of results of the aforementioned test cases proves that the dominant geopotential short periodic (outside of J_2) are the m-daily terms.

Test Case 6 analyzes the impact of expanding the averaged equations of motion for the DSST truth model (other initial conditions for the DSST truth remain the same as in the other test cases):

TEST # 6

Mean Element Equations of Motion

- 12 x 0 zonal harmonics
- J_2^2 terms

Short Periodics

- J_2 terms
- Tesseral M-daily terms (through degree and order 5)

The initial conditions for the least squares fit to this truth trajectory are the same as those for the other test cases. The results of the differential correction runs for the sixth test case are given in Table 7.

Table 7. Test Case 6 PPT2/PPT2-MDAILY DC Results

Parameter	GTDS PPT2 (Original)	GTDS PPT2-MDAILY
Run Time	39.64 sec	38.90 sec
DC RMS	599.60 m	71.06 m
DC Iterations	5	4
Semimajor Axis σ	8.08373 cm	0.964262 cm
Total Position Error RMS 3 Day Fit	614.03 m	72.965 m
Total Position Error RMS 3 Day Predict	661.45 m	243.56 m

These results, when compared to those of Test Case 1, suggest that secular and long period zonal effects spanning J_6 - J_{12} have a non-trivial impact upon the accuracy of a trajectory; approximately 55 meters can be accredited to these terms during the fit span (with an even larger impact in the predict span). Again, if future efforts are undertaken to enhance the accuracy of analytic theories, higher degree secular and long period zonal contributions should be considered.

All the testing described thus far has focused solely on the geopotential. In reality, other perturbations greatly impact near earth trajectories. One of the most dominant (and unpredictable) perturbative effects stems from atmospheric drag. Test Case 7 included drag in the DSST truth model (other initial conditions for the DSST truth remain the same as in the other test cases).

TEST # 7

Mean Element Equations of Motion

- 5 x 0 zonal harmonics

- J_2^2 terms
- Atmospheric drag: Jacchia 70 Density Model ($F_{10.7}$ = 150, Ap = 12, area/mass = 0.01m^2/kg)

Short Periodics

- J_2 terms
- Tesseral M-daily terms (through degree and order 5)
- Atmospheric drag

The initial conditions for the least squares fit to this truth trajectory are the same as those for the other test cases (except that the PPT2 drag parameter M_2 is set to the value of 5.D-8 rad/Herg^2 rather than zero). The results of the differential correction runs for the Test Case 7 are given in Tables 8 and 9.

Table 8. Test Case 7 PPT2/PPT2-MDAILY DC Results (solve for M2)

Parameter	GTDS PPT2 (Original) Solve For M_2 Only	GTDS PPT2-MDAILY Solve For M_2 Only
Run Time	38.29 sec	38.80 sec
DC RMS	594.53 m	50.33 m
DC Iterations	6	4
Semimajor Axis σ	31.3689 cm	2.49692 cm
M_2	0.1128×10^{-6}	0.1123×10^{-6}
M_2 σ	0.187×10^{-9}	0.149×10^{-10}
Total Position Error RMS 3 Day Fit	610.18 m	54.317 m
Total Position Error RMS 3 Day Predict	1596.2 m	1953.6 m

Table 9. Test Case 7 PPT2/PPT2-MDAILY DC Results (solve for M2 and M3)

Parameter	GTDS PPT2 (Original) Solve M_2 and M_3	GTDS PPT2-MDAILY Solve M_2 and M_3
Run Time	38.78 sec	40.92 sec
DC RMS	590.99 m	45.11 m
DC Iterations	6	6
Semimajor Axis σ	77.1743 cm	5.24562 cm
M_2	0.1053×10^{-6}	0.1095×10^{-6}
M_2 σ	0.111×10^{-8}	0.750×10^{-10}
M_3	0.1559×10^{-10}	0.5989×10^{-11}

M_3 σ	0.227×10^{-11}	0.154×10^{-12}
Total Position Error RMS 3 Day Fit	606.80 m	48.328 m
Total Position Error RMS 3 Day Predict	3658.1 m	184.56 m

These results emphasize the dominant effect atmospheric drag has on near-earth satellite orbits; predict span errors and sigmas in semimajor axis are greatly increased. It is interesting to note how much better the GTDS PPT2-MDAILY theory performs than GTDS PPT2 (original) when both drag solve-fors (M_2 and M_3) are used. This effect is indicative of the DC's ability to better separate drag and geopotential effects when more complete force models are included in the perturbation theory. In addition, the solutions for the drag parameters have sigmas at least an order of magnitude smaller for the GTDS PPT2-MDAILY theory. Finally, it should be stressed that this case represents a simulated data study. Specifically, there is no evolution of the atmosphere density parameters during the prediction span. Subsequent analysis with real observational data will further address the impact of atmospheric drag.

Testing of the GTDS PPT2-MDAILY Capability with Truth Data Generated by the GTDS Cowell (Special Perturbations) Theory

The use of truth trajectories generated by Special Perturbation techniques is widely considered the best method of *simulating* real world satellite motion. For this reason, two test cases using Special Perturbation-generated truth data are presented in this section as a cross-check of some of the DSST testing described in the previous section. The first reference orbit includes geopotential effects through the 5^{th} degree and order (no other perturbations are considered). This orbit is created by passing the osculating elements from a one day DSST run

with force models and initial conditions as outlined in Test Case 1 to the GTDS Cowell Orbit Generator (note: the Cowell Orbit Generator uses WGS 72 coefficients and the PPT2 value of the gravitational parameter for this test case). Then, GTDS PPT2 is least squares fit to the Cowell reference orbit over a three day span (since a one day DSST run was required to generate the osculating elements which correspond to the mean elements used in the DSST test cases, the fit span is the 24-27 Feb 82 rather than 23-26 Feb 82). Initial conditions for the DC are given in Table 10.

Table 10. Test Case 8 PPT2/PPT2-MDAILY DC Input Parameters

Parameter	Value	Parameter	Value
Epoch (YYMMDD.0)	820224.0	Epoch (HHMMSS.S)	000000.0
Input Coordinate Frame	GTDS NORAD TEME	Fit Span Length	3 Days
Input Element Type	PPT2 Mean Keplerian	Solve for M_2	No
Semimajor Axis	6834.9 km	Solve for M_3	No
Eccentricity	0.0014	Gravitational Parameter	398597.63 km^3/sec^2
Inclination	64.8 deg	Gravity Model	WGS 72
Longitude of Ascending Node	224.0 deg	M-daily Terms	Through Degree and Order 5
Argument of Perigee	271.0 deg	Position Observation σ	1500 m
Mean Anomaly	216.0 deg	Velocity Observation σ	150 cm/sec
M_2	0.0 rad/$Herg^2$	Integration Coordinate Frame	GTDS NORAD TEME
M_3	0.0 rad/$Herg^3$	Output Coordinate Frame	GTDS Mean of 1950

Results for this test are given in Table 11.

Table 11. Test Case 8 PPT2/PPT2-MDAILY DC Results

Parameter	GTDS PPT2 (Original)	GTDS PPT2-MDAILY
Run Time	37.02 sec	39.77 sec
DC RMS	563.59 m	56.87 m
DC Iterations	5	5
Semimajor Axis σ	7.84019 cm	0.843381 cm
Total Position Error RMS 3 Day Fit	601.31 m	58.274 m
Total Position Error RMS 3 Day Predict	610.79 m	81.176 m

As expected, these results very closely follow those of Test Case 5 (not included in this document for the sake of brevity), which used DSST's best emulation of a 5x5 Special Perturbations technique. These results can also be compared with Test Case 3 (Table 6). Slight differences are found in the predict span (Test Case 5's errors in the predict span were roughly 25 meters smaller than those given in Table 11), mainly due to truncations in the DSST short periodic model. The particular configurations for the short periodic generator were selected at run time and, if necessary, could be configured to include more complete modeling. This increased modeling, however, would be gained at the expense of computational efficiency.

The second Cowell test case (Test Case 9) added atmospheric drag to the first Cowell test case (Harris-Priester density model with $F_{10.7}$ = 150). All other test parameters were the same as in the first Cowell case (*a priori* M_2 value = 5.D-8, M_3 = 0). The results are given in Tables 12 and 13.

Table 12. Test Case 9 PPT2/PPT2-MDAILY DC Results (solve for M2)

Parameter	GTDS PPT2 (Original) Solve For M_2 Only	GTDS PPT2-MDAILY Solve For M_2 Only
Run Time	38.12 sec	40.87 sec
DC RMS	575.75 m	94.11 m
DC Iterations	5	5
Semimajor Axis σ	30.5859 cm	4.88109 cm
M_2	0.1031×10^{-6}	0.1026×10^{-6}
M_2 σ	0.182×10^{-9}	0.291×10^{-10}
Total Position Error RMS 3 Day Fit	598.35 m	100.32 m
Total Position Error RMS 3 Day Predict	2009.9 m	2435.9 m

Table 13. Test Case 9 PPT2/PPT2-MDAILY DC Results (solve for M2 and M3)

Parameter	GTDS PPT2 (Original) Solve M_2 and M_3	GTDS PPT2-MDAILY Solve M_2 and M_3
Run Time	38.06 sec	39.76 sec
DC RMS	570.54 m	88.28 m
DC Iterations	5	5
Semimajor Axis σ	74.8626 cm	11.0891 cm
M_2	0.9501×10^{-7}	0.9869×10^{-7}
M_2 σ	0.107×10^{-8}	0.159×10^{-9}
M_3	0.1692×10^{-10}	0.8088×10^{-11}
M_3 σ	0.220×10^{-11}	0.326×10^{-12}
Total Position Error RMS 3 Day Fit	594.48 m	93.015 m
Total Position Error RMS 3 Day Predict	3657.8 m	355.75 m

These results show the same trends evident in Test Case 7. Note that different atmosphere density models are used in the two test cases so exact agreement is not expected. GTDS PPT2 MDAILY greatly outperforms GTDS PPT2 when solutions for M_2 and M_3 are obtained. Again, original PPT2 (without the m-dailies) performs worse when solving for both drag parameters than it does when solving only for M_2.

Testing of the GTDS PPT2-MDAILY Capability where the Truth Orbits are Actual Orbits

The results discussed thus far have focused on the processing of simulated data generated by truth models configured for orbital dynamics similar to those contained in PPT2 and PPT2-MDAILY. The ultimate test of a propagation theory is its performance with regard to observational data generated by real world tracking techniques (i.e., skin-track observations, transponder data, etc.). It becomes extremely difficult, however, to maintain controlled conditions in testing of this nature; clock errors, quantity of observations, orbital dispersion of observations, and biases and standard deviations in the tracking data which are station dependent are just a few of the problems which must be considered when processing real world data. In addition, the question of "what is truth?" must be addressed. In the past, attempts to maintain controlled testing conditions (which provide insight on the pure limitations of the physical modeling in a perturbation theory) have centered around using special perturbations techniques with the best available force models for truth trajectories.

Recently, the development of Precise Orbit Ephemeris (POE) data for spacecraft equipped with satellite laser retro-reflectors, GPS receivers, or other precise onboard navigation equipment has led to a break-through in the manner in which perturbation theories are tested. The POE data is comprised of Earth-centered, Earth-fixed (ECEF) position and velocity vectors on a regularly spaced time grid over the entire orbit. One example, the TOPEX POE, results from accurate, temporally dense, and globally distributed tracking data (satellite laser ranging and DORIS receiver) processed with improved force models through a combined effort of individuals at NASA GSFC, CNES, and the University of Texas at Austin (Ref. 19). Other POE solutions, such as those for TAOS (Ref. 20) are based on differential GPS processing. The accuracy of these POE solutions can be summarized as follows (Refs. 19 and 20):

- TOPEX ~ 15 cm

- TAOS ~ 3 m

The TAOS orbit is of particular importance since it is around 500 km and significantly perturbed by atmospheric drag.

In this section, the results of processing the TOPEX and TAOS POE solutions with GTDS PPT2 and GTDS PPT2-MDAILY will be presented. The steps in the test procedure are as follows:

1. Least squares fit GTDS PPT2 and GTDS PPT2-MDAILY to the POE solutions using the first position and velocity set in the POE file as an *a priori* guess for the DC

2. Generate a trajectory based on the DC solve-for parameter list for both GTDS PPT2 and GTDS PPT2-MDAILY (output data points on a time grid corresponding to the POE solutions)

3. Compare the original POE data points to the data points generated with the best fit trajectory (see Ref. 21, Appendix C for a description of the MatLab procedures).

TOPEX DATA

The data interval for this test is the December 1992 span studied in Ref. 21. Since TOPEX is at an altitude greater than 1300 km, no attempt was made to solve for drag parameters. Results for a fit span length slightly less than five (5) days are presented in Table 14. In this case, the Tesseral M-daily portion of the PPT2-MDAILY theory was configured to use the 12 x 12 portion of the WGS-72 geopotential.

Table 14. TOPEX POE Test Case: PPT2/PPT2-MDAILY DC Results

Parameter	GTDS PPT2 (Original)	GTDS PPT2-MDAILY
Run Time	n/a	n/a
DC RMS	394.4 m	162.965 m
DC Iterations	6	4
Semimajor Axis σ	1.3 cm	0.52 cm

Side by side comparisons between PPT2 and PPT2-MDAILY are given in Figures 4 through 9 for several parameters:

- radial differences Vs the POE
- cross track differences Vs the POE
- along track differences Vs the POE
- semi major axis/eccentricity differences Vs the POE
- inclination/node differences Vs the POE
- argument of latitude differences Vs the POE

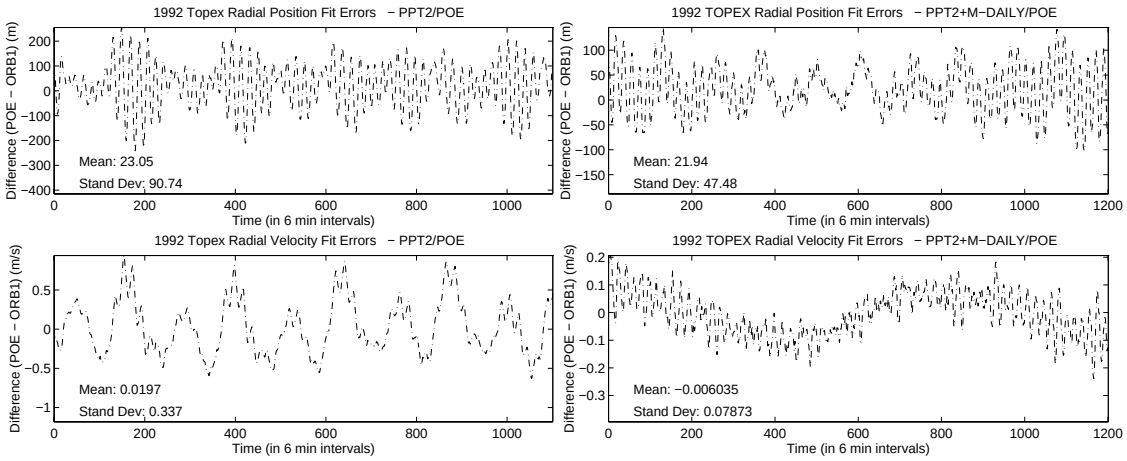

Figure 4. TOPEX Radial Differences vs. POE (PPT2 and PPT2-MDAILY)

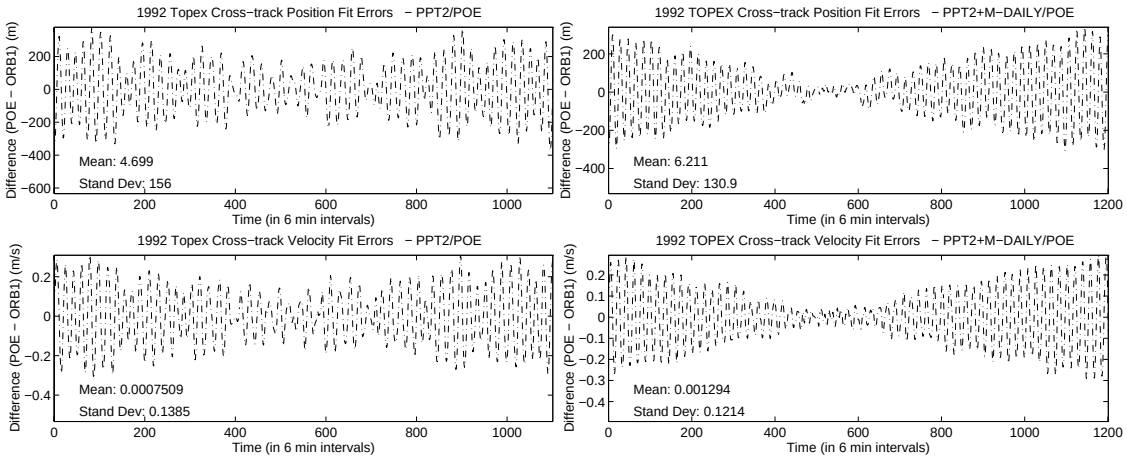

Figure 5. TOPEX Cross Track Differences vs. POE (PPT2 and PPT2-MDAILY)

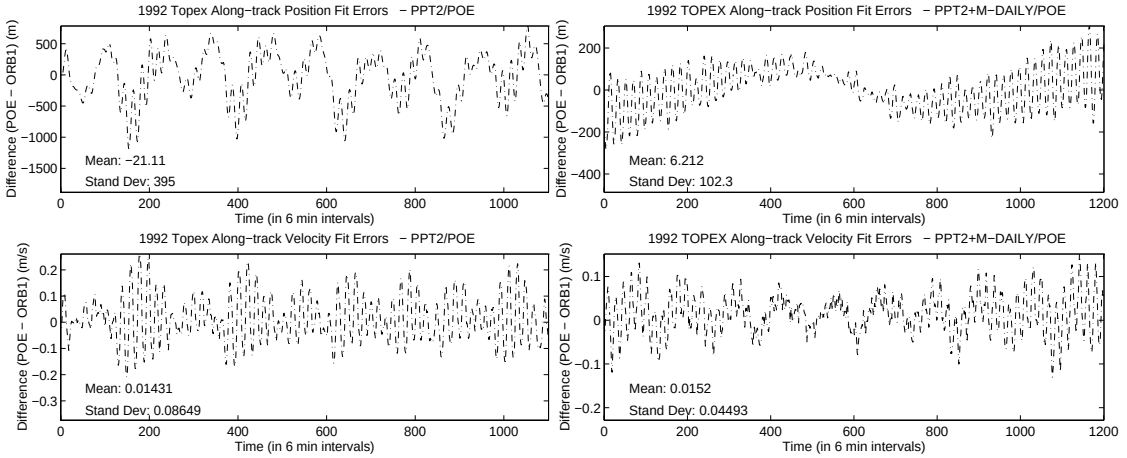

Figure 6. TOPEX Along Track Differences vs. POE (PPT2 and PPT2-MDAILY)

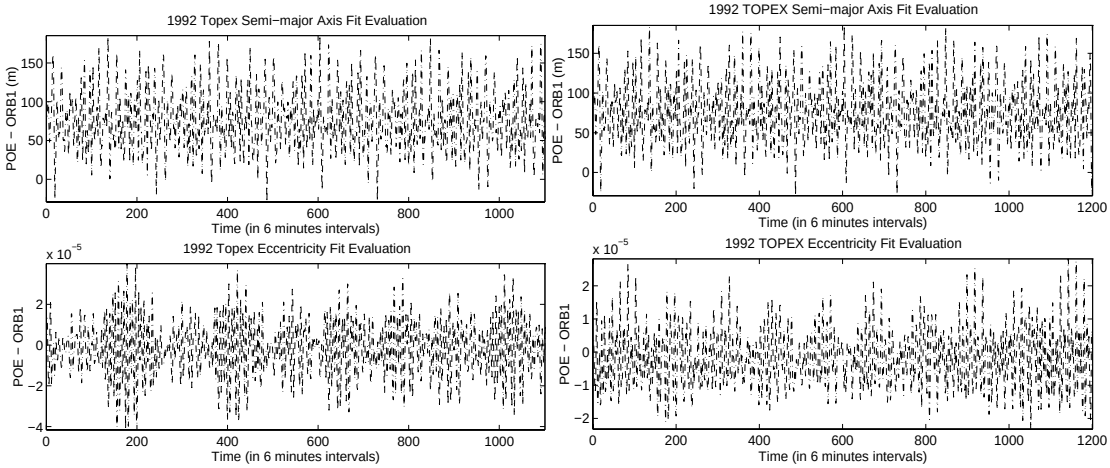

Figure 7. TOPEX Semi major axis/ecc Differences vs. POE (PPT2 and PPT2-MDAILY)

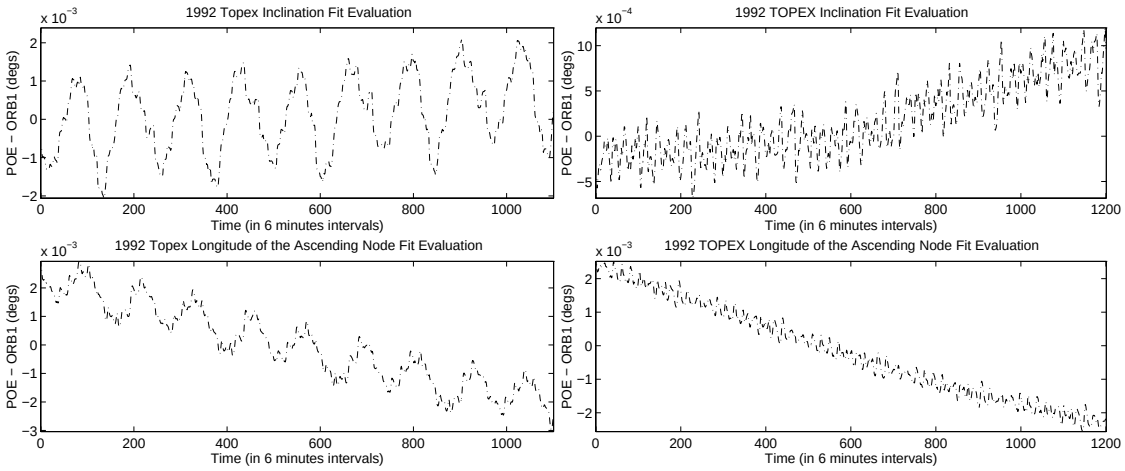

Figure 8. TOPEX inclination/node Differences vs. POE (PPT2 and PPT2-MDAILY)

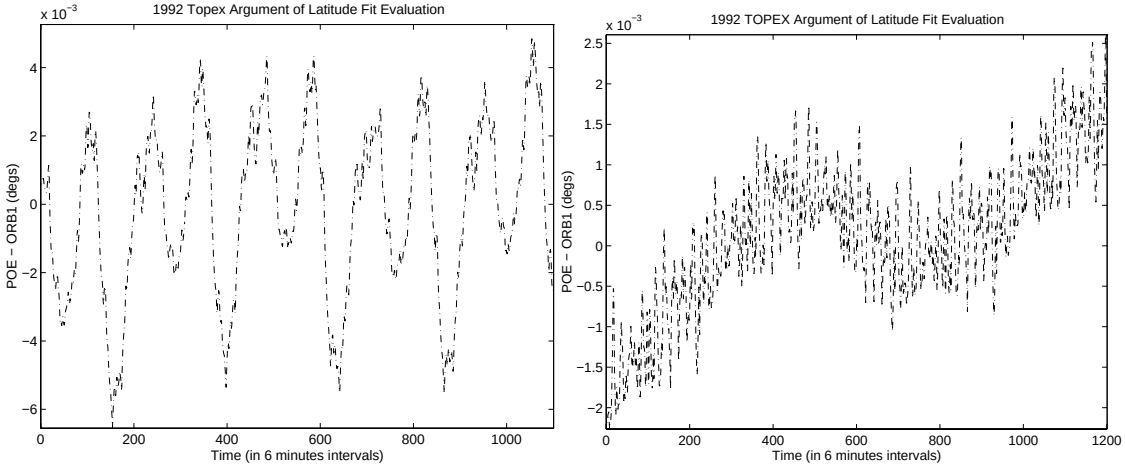

Figure 9. TOPEX argument of latitude Differences vs. POE (PPT2 and PPT2-MDAILY)

Almost all of the plots demonstrate the improved accuracy of PPT2-MDAILY with the DC RMS being reduced from nearly 395 m to about 163 m (Table 14). We note also that convergence is achieved in a smaller number of iterations. The reduction of the tesseral m-daily signature in PPT2 plots makes the systematic nature of the remaining residual more apparent. The cross track and along track position difference plots, as well as the inclination, LAN, and argument of latitude element difference plots all demonstrate this phenomena. The clear secular/long-periodic signature in the inclination and LAN plots supports consideration of further

improvements to that portion of the theory. Review of the GTDS Compare plots produced by simulated data Test Case 6 (Table 7) suggests that at least a portion of the remaining PPT2-MDAILY LAN difference in Figure 8 is due to unmodeled zonal secular/long period motion. Finally, the semi major axis plots (Figure 7) are unchanged with PPT2-MDAILY; this is to be expected because (from analytical considerations) the tesseral m-daily terms cause no periodic motion in the semi major axis. These semi major axis residuals are due in part to the unmodeled tesseral linear combination terms [see plots associated with simulated data Test Case 3 (Table 6)].

TAOS DATA

The data interval for this test is 28 May to 2 June 1994, during which the atmosphere is moderately disturbed (average Kp value of 4). Since TAOS is at a much lower altitude than TOPEX (roughly 500 km), the PPT2 and PPT2 M-DAILY solve-for vectors included the drag parameter. M-daily terms through degree and order 12 were exercised in the development of the Fourier coefficients for the short periodic effects. Results for a four day fit span length are presented in Table 15. Additional experiments with shorter fit spans are in progress at the time of this draft.

Table 15. TAOS POE Test Case: PPT2/PPT2-MDAILY DC Results

Parameter	GTDS PPT2 (Original)	GTDS PPT2-MDAILY
Run Time	n/a	n/a
DC RMS	626.99 m	144.99 m
DC Iterations	5	4
Semimajor Axis σ	5.77 cm	1.33 cm
M_2	0.3616D-8	0.3648D-8
M_2 σ	0.198D-10	0.457D-11
M_3	n/a	n/a
M_3 σ	n/a	n/a

Side by side comparisons between PPT2 and PPT2-MDAILY are given in Figures 10 through 15 for the following parameters:

- radial differences Vs the POE
- cross track differences Vs the POE
- along track differences Vs the POE
- semi major axis/eccentricity differences Vs the POE
- inclination/node differences Vs the POE
- argument of latitude differences Vs the POE

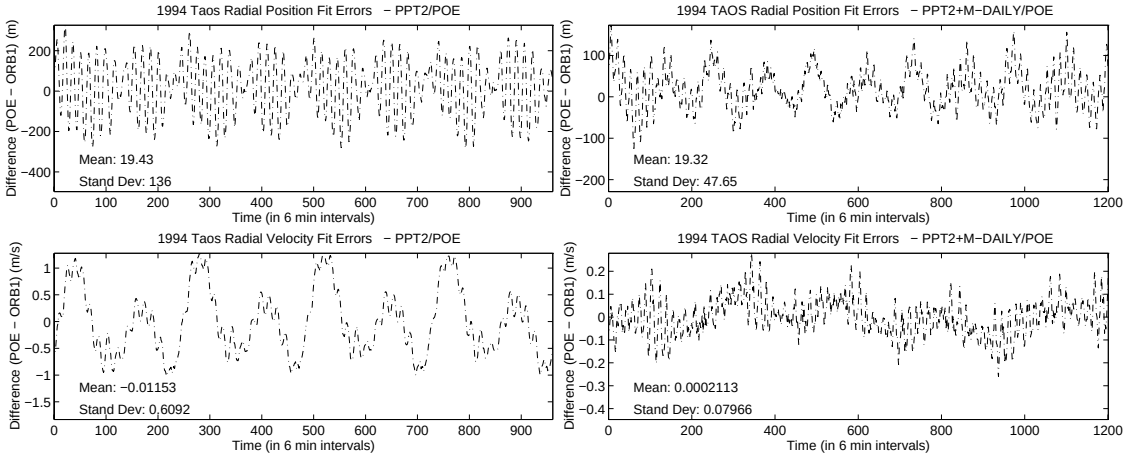

Figure 10. TAOS Radial Differences vs. POE (PPT2 and PPT2-MDAILY)

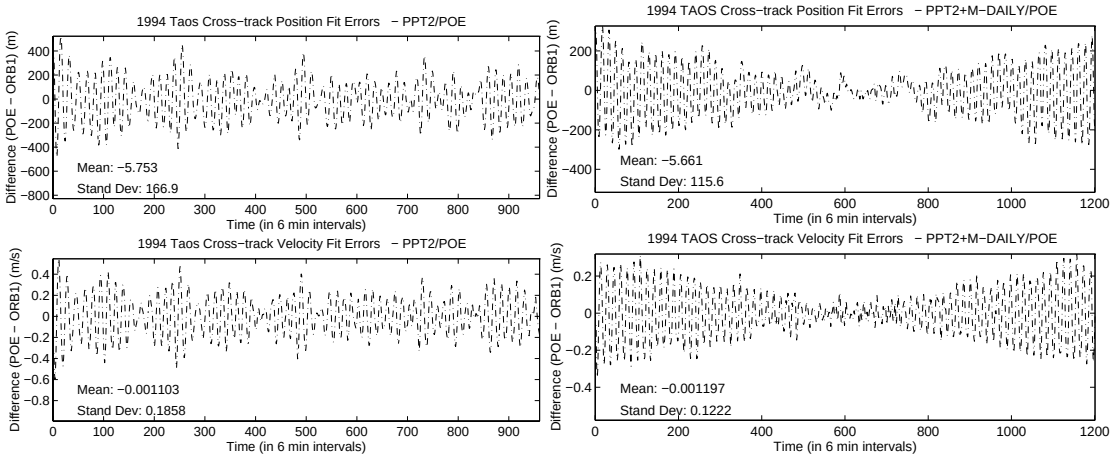

Figure 11. TAOS Cross Track Differences vs. POE (PPT2 and PPT2-MDAILY)

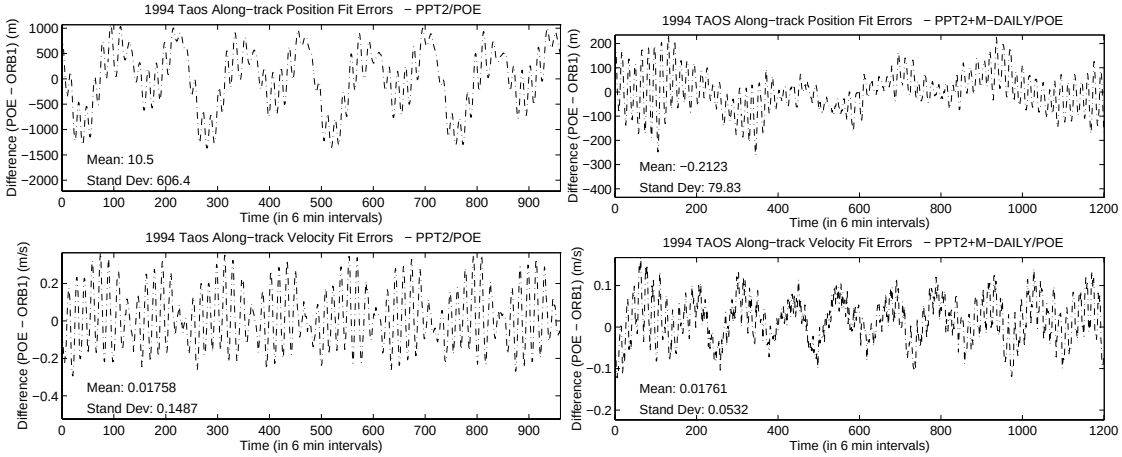

Figure 12. TAOS Along Track Differences vs. POE (PPT2 and PPT2-MDAILY)

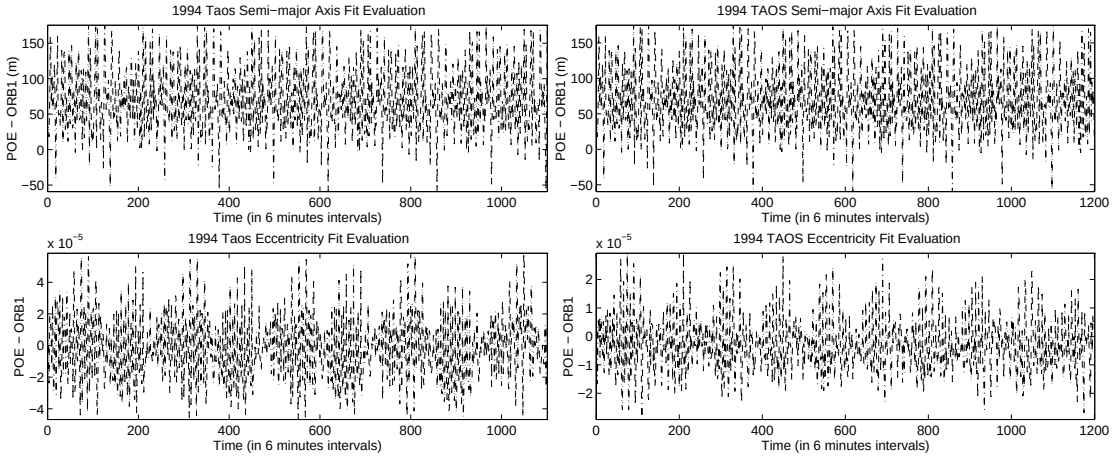

Figure 13 TAOS Semi major axis/ecc Differences vs. POE (PPT2 and PPT2-MDAILY)

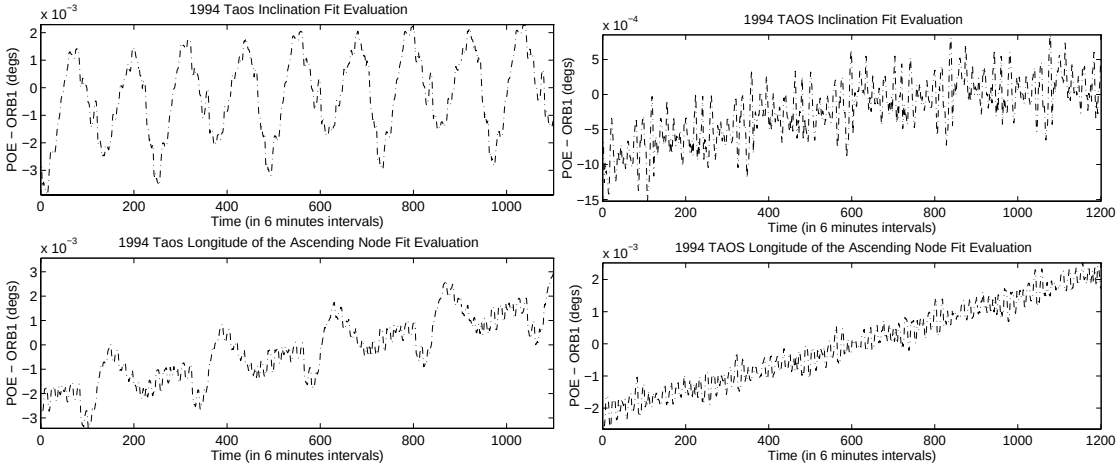

Figure 14. TAOS inclination/node Differences vs. POE (PPT2 and PPT2-MDAILY)

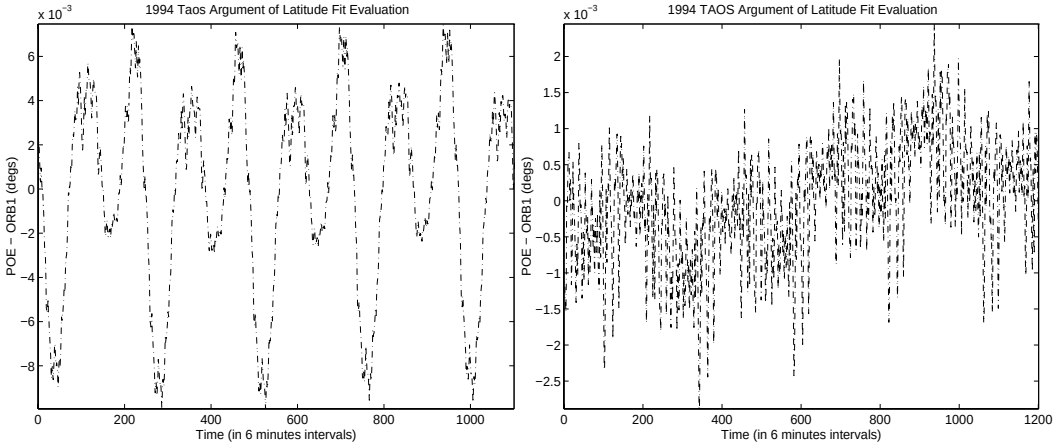

Figure 15. TAOS argument of latitude Differences vs. POE (PPT2 and PPT2-MDAILY)

The primary observations from the TOPEX data also apply to the TAOS results given in Figures 10 to 15:

- almost all the PPT2-MDAILY plots demonstrate improved accuracy vs. PPT2
- the remaining PPT2-MDAILY residuals have a more systematic structure
- the a/e plots (Figure 13) exhibit high frequency residuals in part due to tesseral linear combination terms
- the PPT2-MDAILY DC converges in a smaller number of iterations

Uniquely with TAOS, it is observed that:

- the PPT2 m-dailies have a larger along track magnitude with TAOS than with TOPEX
- the along track PPT2-MDAILY position residuals (Figures 12 and 15) exhibit a less systematic variation than those for TOPEX (Figures 6 and 9) perhaps reflecting the disturbed atmosphere conditions
- the sigma for the M2 drag solve-for parameter is much smaller for PPT2-MDAILY than for PPT2

CONCLUSIONS AND FUTURE WORK

The Draper Semianalytic Satellite Theory's tesseral m-daily model has been successfully attached to the GTDS version of PPT2. Testing of the GTDS PPT2-MDAILY theory against both simulated data (generated by DSST semianalytic and Cowell special perturbation techniques) and real data (in the form of TOPEX and TAOS POE solutions) provides accuracy improvements of several hundred meters as compared to the current operational version of PPT2. In addition, 12 and 24 hour frequency oscillations which are highly visible in residual plots comparing trajectories of PPT2 least squares fits to high accuracy POE solutions are removed with the inclusion of the tesseral m-daily terms.

There are opportunities for further enhancement of the PPT2-MDAILY theory. Specifically, two classes of terms have the potential to further improve the accuracy:

- secular and long periodic terms due to the zonal harmonics that are presently unmodeled (J6 and above)
- tesseral linear combination short periodic terms

Inclusion of the zonal terms would be aided by the availability of a recursive form of Brouwer's core algorithms for the secular and long-periodic motion. For the tesseral linear combination short periodic terms, there is already a recursive model available from the DSST development (Ref. 12). The interface between PPT2 and the tesseral linear combination terms would employ much of the capability already developed for the tesseral m-dailies.

So far we have focused on enhancing the capabilities of PPT2. However, there are other 'operational' implementations of the Brouwer and Brouwer-Lyddane theories that might benefit from this approach. The GP4 theory (Ref. 3) and the HANDE theory (Ref. 18) are two examples.

The development of enhanced GP theories is compatible with the idea of an 'open' space object element set catalog that could support both long period predictions with the DSST as well as the usual short arc GP operations. Such an 'open' space object catalog might be quite useful in an environment with increased numbers of LEO payloads.

ACKNOWLEDGMENTS

The authors would like to thank Ron Proulx and Rick Metzinger of the Draper Laboratory, Lt. Scott Carter (USAF/MIT/Draper), and Lt. Naresh Shah (USAF/MIT/Draper) who contributed their expertise. The authors would like to thank Steve Knowles and Paul Schumacher of the Naval Space Command for the availability of the PPT2 code and for several useful discussions. The authors would also like to acknowledge the encouragement of Col. S. Alfano (now at USAF N/SP AN in Colorado Springs) and Maj. Dave Vallado at the USAF Phillips Laboratory Astrodynamics Division (PL/VTA), and Beny Neta at the Naval Postgraduate School. Finally, the first author would like to acknowledge his former colleague, Mr. Leo Early, for the re-usable design of the GTDS package for managing the DSST short periodic coefficient interpolators.

REFERENCES

1. "PPT2: The NAVSPASUR Model of Satellite Motion," NAVSPASUR Report 92-01, July 1992. Available from Commander, NAVSPACECOM, 5280 Fourth Street, Dahlgren, VA 22448-5300; attention: Logistics and Information Systems Division (Mail Code N4/6).

2. Schumacher, Paul W. Jr., and Robert A. Glover, "Analytical Orbit Model for the U. S. Naval Space Surveillance: An Overview", AAS Pre-print 95-427, presented at the AAS/AIAA Astrodynamic Specialist Conference, Halifax, Nova Scotia, Canada, 14-17 August 1995.

3. Hoots, Felix R., and Roehrich, Ronald L., Models for Propagation of NORAD Element Sets, Spacetrack Report No. 3, December 1980, Aerospace Defense Command, United States Air Force.

4. Knowles, Stephen H., "A Comparison of Geocentric Propagators for Operational Use," AAS Pre-print 95-429, presented at the AAS/AIAA Astrodynamic Specialist Conference, Halifax, Nova Scotia, Canada, 14-17 August 1995.

5. Hujsak, Richard S., A Restricted Four Body Solution for Resonating Satellites Without Drag, Spacetrack Report No. 1, November 1979, Aerospace Defense Command, United States Air Force.

6. Glover, Robert A., and Paul W. Schumacher Jr., "Testing of the Naval Space Command New Analytic Orbit Model," AAS Pre-print 95-430, presented at the AAS/AIAA Astrodynamic Specialist Conference, Halifax, Nova Scotia, Canada, 14-17 August 1995.

7. Coffey, Shannon L., Harold L. Neal, Alan M. Segerman, and Jeffrey J. Travisano, "An Analytic Orbit Propagation Program for Satellite Catalog Maintenance," AAS Pre-print 95-426, presented at the AAS/AIAA Astrodynamic Specialist Conference, Halifax, Nova Scotia, Canada, 14-17 August 1995.

8. Coffey, S. L., H. L. Neal, E. Jenkins, and H. Reynolds, "Parallel Processing of Uncorrelated Observations into Satellite Orbits," AAS Pre-print 96-146, presented at the AAS/AIAA Spaceflight Mechanics Meeting, Austin TX, 12-15 February 1996.

9. Cefola, P. J., D. J. Fonte, and N. Shah, "The Inclusion of the Naval Space Command Satellite Theory PPT2 in the R&D GTDS Orbit Determination System," AAS Pre-print 96-142, presented at the AAS/AIAA Spaceflight Mechanics Meeting, Austin, Texas, February 1996.

10. Tapley, B. D., et al, "Precision Orbit Determination for TOPEX/POSEIDON," Journal of Geophysical Research, Vol. 99, No. C12, pp. 24,383-24,404, December 15, 1994.

11. Guinn, J., B. Williams, P. Wolff, R. Fennessey, and T. Wiest, "TAOS Orbit Determination Results Using Global Positioning Satellites," AAS Pre-Print 95-146, presented at the AAS/AIAA Spaceflight Mechanics Meeting, Albuquerque NM, February 1995.

12. Proulx, R. J., W. D. McClain, L. W. Early, and P. J. Cefola, "A Theory for the Short-Periodic Motion Due to the Tesseral Harmonic Gravity Field," AAS Paper 81-180, AAS/AIAA Astrodynamics Specialist Conference, Lake Tahoe NV, August 1981.

13. Brouwer, Dirk, "Solution of the Problem of Artificial Satellite Theory Without Air Drag," Astronomical Journal, Vol. 64 pp. 378-397, 1959.

14. Lodato, M. W., and J. B. Fraser, An Introduction to the Brouwer Theory, MITRE Corporation, Working Paper W-07487/0000/00/0/00 (Contract No.: AF19(628)2390), January 25, 1965.

15. Lane, M. H., and K. H. Cranford, "An Improved Analytical Drag Theory for the Artificial Satellite Problem," AIAA Paper 69-925, AIAA/AAS Astrodynamics Conference, Princeton, NJ, August 1969.

16. Liu, J. F., and R. L. Alford, "A Semi-Analytic Theory for the Motion of a Close-Earth Artificial Satellite with Drag," AIAA Paper 79-0123, 17th Aerospace Sciences Meeting, New Orleans, LA, January 1979.

17. Hoots, F. R., "A Short Efficient Analytical Satellite Theory," J. Guidance and Control, Vol. 5, No. 2, pp. 194-199, March-April 1982.

18. Hoots, F. R., and R. G. France, "An Analytic Satellite Theory Using Gravity and a Dynamic Atmosphere," Celestial Mechanics, Vol. 40, No. 1, pp 1 -18, 1987.

19. Tapley, B. D., et al, "Precision Orbit Determination for TOPEX/POSEIDON," Journal of Geophysical Research, Vol. 99, No. C12, pp. 24,383-24,404, December 15, 1994.

20. Guinn, J., B. Williams, P. Wolff, R. Fennessey, and T. Wiest, "TAOS Orbit Determination Results Using Global Positioning Satellites," AAS Pre-Print 95-146, presented at the AAS/AIAA Spaceflight Mechanics Meeting, Albuquerque NM, February 1995.

21. Carter, Scott S., Precision Orbit Determination From GPS Receiver Navigation Solutions, Master of Science Thesis. Department of Aeronautics and Astronautics, Massachusetts Institute of Technology. CSDL-T-1086. June 1996.